

# Colour Strings vs. Hard Pomeron in Perturbative QCD

M.A.Braun<sup>a,b</sup> and C.Pajares<sup>a</sup>

<sup>a</sup> Dep. of Elementary Particles,

Univ. of Santiago de Compostela, 15706, Santiago de Compostela, Spain,

<sup>b</sup> Dep. of High Energy physics, University of S.Petersburg,  
198504 S.Petersburg, Russia

November 3, 2018

**Abstract.** Average multiplicities and transverse momenta in AA collisions at high energies are studied in the soft and hard regions, in fusing string and perturbative QCD scenarios respectively. Striking similarities are found between the predictions of the two approaches. Multiplicities per string and average  $p_T^2$  are found to, respectively, drop and rise with  $A$  in a very similar manner, so that their product is nearly a constant. In both approaches total multiplicities grow as  $A$ , that is, as the number of participants. The high tail of the  $p_T$  distribution in the perturbative QCD scenario is found to behave  $\propto A^{1.1}$ .

## 1 Introduction

At present multiparticle production at high energies is described by different models, which are supposed to be valid in different intervals of transverse momenta of secondaries. At small momenta (soft region) one of the most popular and successful models is the colour string model. In its original formulation it assumes that in a collision a certain number of colour strings of definite length in rapidity are stretched between the colliding partons, which then independently decay into observed secondaries [1, 2]. The colour string is visualized as a strong colour field which is successively broken by creation of quark-antiquark pairs. A more refined version takes into account not only a finite length in rapidity but also a finite transverse dimension of the string. This inevitably leads to the phenomenon of string fusion and percolation [3, 4, 5]. The colour string model with fusion and percolation describes quite satisfactorily multiparticle production in the soft region. In particular, it predicts that, due to fusion, multiplicities become substantially damped, as compared to the independent string picture. The damping factor  $F$  may be related to the so-called percolation parameter

$$\eta = \frac{N\sigma_0}{S}, \quad (1)$$

where  $\sigma_0$  is the transverse area of the string and  $N$  is the number of strings in the interaction area  $S$ . As a function of  $\eta$  one finds for the damping factor [5]

$$F(\eta) = \sqrt{\frac{1 - e^{-\eta}}{\eta}}, \quad (2)$$

so that at large  $\eta$  multiplicities are damped by  $1/\sqrt{\eta}$ .

With all this, the colour string model remains mostly phenomenological, although at the basis of it there lie certain ideas borrowed both from the old Regge phenomenology and QCD in the limit of large number of colours (see [1]). Less phenomenological approaches can naturally be developed in the hard region where the secondaries are assumed to have large transverse momenta. The well known hard scattering picture has been successfully applied to production of heavy flavour and high-mass Drell-Yan pairs. However this approach is valid only in the kinematical region appropriate for the DGLAP evolution, for values of  $x$  of the order unity, and the following ordering in transverse momenta. The region of small  $x$  can be reached via the evolution according to the BFKL equation and its generalization for nuclei. Both hard approaches suffer from serious drawbacks. The DGLAP evolution cannot be generalized to several hard collisions in a convincing manner, since this involves multiparton distributions corresponding to higher twists. The BFKL approach does not take into account the running of the coupling. It also involves small transverse momenta, where it cannot be valid, and violates unitarity for hadronic scattering. In this respect the situation is better for scattering off nuclei, where the small transverse momentum region is strongly damped and unitarity is automatically fulfilled [6, 7]. In spite of these difficulties hard approaches give predictions which are compatible with the experimental data.

In view of this split between soft and hard regions it is of certain interest to find a bridge between them. In particular it has long been suspected that damping of multiplicities predicted by colour string fusion has its obvious counterpart in the hard region in the form of pomeron fusion due to pomeron interaction. Note that a literal comparison between the two approaches is hardly possible. In the colour string picture fusion leads to appearance of parts of the transverse space with a larger colour field strength ("strings of higher colour"). As a result, damping of multiplicities is accompanied by the rise of the average transverse momentum. In the pomeron picture, at least in the high colour limit, fusion of pomerons does not lead to new objects. Only the average number of pomerons may become reduced, and the multiplicities with them. But one does not naively expect any change in the transverse momentum. As we shall see in the following sections, this is fully confirmed in the simple old-fashioned local supercritical pomeron model, in which also damping of the multiplicities is found to be much stronger than predicted by the colour string models with fusion. The new result reported in this paper is that the perturbative QCD hard pomeron approach leads to multiparticle production which qualitatively fully agrees with the colour string approach with fusion. Not only damping of the multiplicities turns out to be of the same strength as in the string picture, but also the average transverse momenta are found to rise nearly as predicted by the latter model. So we find an agreement between predictions of these two models, pertaining to completely different (in fact opposite) kinematical regions of secondaries, about certain basic features of multiparticle spectra. These results are not fully unexpected. Indeed similar predictions were found previously [8] in the framework of colour glass condensate [9]. Also in all considered approaches scaling in the transverse momentum distribution was observed [8, 10, 11]. We consider this as a strong support for these predictions and thereby for the models.

## 2 Generalities. Fusing colour string predictions

Our basic quantity will be the inclusive cross-section  $I_{AB}(y, k)$  to produce a particle with the transverse momentum  $k$  at rapidity  $y$  in a collision of two nuclei with atomic numbers  $A$  and  $B$ :

$$I_{AB}(y, k) = \frac{(2\pi)^2 d\sigma}{dy d^2k}. \quad (3)$$

It can be represented as an integral over the impact parameter  $b$ :

$$I_{AB}(y, k) = \int d^2b I_{AB}(y, k, b). \quad (4)$$

To simplify our study we shall concentrate on the inclusive cross-section at fixed impact parameter  $b$ . We shall also limit ourselves to collision of identical nuclei  $A = B$  and for brevity denote  $I_{AA} \equiv I_A$  and so on. The corresponding multiplicity at fixed rapidity  $y$  will be given by

$$\mu_A^{tot}(y, b) = \frac{1}{\sigma_A(b)} \int \frac{d^2k}{(2\pi)^2} I_A(y, k, b), \quad (5)$$

where  $\sigma_A(b)$  is the total inelastic cross-section for the collision of two identical nuclei at fixed impact parameter  $b$ . To study the effect of string fusion we shall be interested in the multiplicity per string  $\mu_A(y, b)$ , given by the ratio of (5) to the number of strings  $\nu_A(b)$  at impact parameter  $b$

$$\mu_A(y, b) = \frac{\mu_A^{tot}(y, b)}{\nu_A(b)}. \quad (6)$$

The latter can be determined by the number of inelastic NN collisions times the number of strings in a single NN collision  $\nu_N$ . For identical nuclei we find

$$\nu_A(b) = \frac{A^2 \sigma_N T_{AA}(b)}{\sigma_A(b)} \nu_N \quad (7)$$

where  $T_{AA}(b)$  is the nuclear transverse density in the overlap area:

$$T_{AA}(b) = \int d^2c T_A(c) T_A(b - c), \quad (8)$$

$\sigma_N$  is the NN total cross-section and  $T_A(b)$  is the standard nuclear profile function for a single nucleus  $A$  normalized to unity. In the ratio (6) the total nucleus-nucleus cross-section  $\sigma_A(b)$  cancels;

$$\mu_A(b) = \frac{\int (d^2k / (2\pi)^2) I_A(y, k, b)}{A^2 T_{AA}(b) \sigma_N \nu_N}. \quad (9)$$

This point is very important, since it means that we shall have to calculate only the inclusive cross-sections for the collision of two nuclei but not the total cross-sections, which is a problem of incomparably more complexity.

To simplify the problem still further, we shall consider the simplest choice of constant profile function  $T_A(b)$  inside a circle of nuclear radius  $R_A = A^{1/3} R_0$ . Then also the inclusive cross-section will be independent of  $b$  inside the overlap area. We choose  $b = 0$  (central collision) when the overlap area coincides with the nuclear transverse area to find from (9)

$$\mu_A = A^{-4/3} \frac{\pi R_0^2}{\sigma_N \nu_N} \int \frac{d^2k}{(2\pi)^2} I_A(y, k). \quad (10)$$

Parallel to this we shall study the average transverse momentum squared, defined by

$$\langle k^2 \rangle_A = \frac{\int d^2k k^2 I_A(y, k)}{\int d^2k I_A(y, k)}. \quad (11)$$

Here  $b = 0$  is implied. Equations (10) and (11) will be our basic tools in the following.

We start with the fusing colour strings picture. In it the strength of fusion is determined by the percolation parameter (1). For central collisions it is given by

$$\eta_A = A^{2/3} \frac{\sigma_N^2}{\pi^2 R_0^4 \sigma_A(b=0)} \eta_N, \quad (12)$$

where  $\eta_N$  is the value of the parameter for  $NN$  collisions at the same energy. Note that the value of  $\eta$  depends on the total inelastic nuclear cross-section for central collisions. We take it in the optical approximation as

$$\sigma_A(b=0) = 1 - e^{-A^{4/3} \sigma_N / (\pi R_0^2)}. \quad (13)$$

As stated in the Introduction, the fusing string picture predicts that multiplicities are damped by the factor (2):

$$\mu_A = \mu_0 F(\eta_A) \quad (14)$$

where  $\mu_0$  is the multiplicity corresponding to a single string. From this we find

$$\frac{\mu_A}{\mu_1} = \sqrt{\frac{\eta_1}{\eta_A}} \sqrt{\frac{1 - e^{-\eta_A}}{1 - e^{-\eta_1}}}. \quad (15)$$

This relation describes the  $A$ -dependence of the multiplicity. It does not involve the unknown string multiplicity  $\mu_0$ . At high string densities and consequently large  $\eta$ 's it obviously predicts damping of multiplicities according to

$$\mu_{AA} \propto \frac{1}{\sqrt{\eta_A}} \propto A^{-1/3}. \quad (16)$$

Note that, as a result of fusion, the total multiplicity from being proportional to a number of inelastic collisions,  $\propto A^{4/3}$ , reduces to become proportional to the number of participants  $\propto A$ .

It also follows from the fusing string picture that  $\langle k^2 \rangle_A$  behaves inversely to multiplicity. It grows with  $\eta$ :

$$\langle k^2 \rangle_A = \langle k^2 \rangle_0 \frac{1}{F(\eta_A)}, \quad (17)$$

so that the product  $\mu_A \langle k^2 \rangle_A$  does not change with fusion of strings.

### 3 Old-fashioned local supercritical pomeron

In this section we shall compare predictions about the average multiplicity and transverse momentum which follow from the colour string model with those from the old supercritical local pomeron model. This will serve as a benchmark for the study in the next section of analogous predictions following from the non-local perturbative QCD pomeron.

As shown in [12], if the nucleus-nucleus interaction is governed by the exchange of pomerons with the triple pomeron interactions, the inclusive cross-sections are given by the convolution of two sets of fan diagrams connecting the emitted particle to the two nuclei times the vertex for the emission (Fig. 1). Explicitly, at a given impact parameter  $b$

$$I_{AB}(y, k, b) = f(k) \int d^2c \Phi_B(Y - y, b - c) \Phi_A(y, c), \quad (18)$$

where  $f(k)$  is the emission vertex,  $\Phi_{A,B}$ 's are sums of fan diagrams connected to nuclei A and B and it is assumed that nucleus A is at rest and the incident nucleus B is at the overall rapidity  $Y$ .

The form (18) characteristic for the old-fashioned local Regge-Gribov theory immediately tells us that the average transverse momentum does not depend on  $A$  or  $B$  and so does not feel fusion of pomerons at all. It obviously follows from the fact that independent of  $A$  or  $B$  the observed particle is emitted from the same single pomeron. Therefore predictions of the old local pomeron theory for the transverse momentum dependence do not agree with those from the fusing colour string model. They rather correspond to models without fusion, in which indeed  $\langle k^2 \rangle$  does not depend on the string density.

Passing to the multiplicities we use the well-known solution for the fans [13]. Taking  $A = B$  and constant nuclear profile functions we have for  $|b| < R_A$

$$\Phi_A(y) = A^{1/3} \frac{g}{R_0^2} \frac{e^{\Delta y}}{1 + A^{1/3} \frac{\lambda}{R_0^2 \Delta} (e^{\Delta y} - 1)}, \quad (19)$$

where  $\Delta$  is the pomeron intercept minus one,  $\lambda$  (positive) is the triple pomeron coupling with a minus sign and  $g$  is the pomeron nucleon coupling. Taking  $y = Y/2$  (central rapidity) we find the inclusive cross-section defined in the previous section as

$$I_A(y, k) = A^{2/3} \pi R_0^2 f(k) \left[ \Phi_A \left( \frac{Y}{2} \right) \right]^2 \quad (20)$$

The  $A$ -dependence of this inclusive cross-section obviously depends on the energy. At small energies one may neglect the second term in the denominator of (19), which actually means that one neglects all non-linear effects. Then  $J_A \propto A^{4/3}$  and from (10) one concludes that the multiplicity per string does not depend on  $A$ , as expected. At large enough  $Y$  when one can retain only the exponential term in the denominator of (19) the inclusive cross-section  $I_A$  becomes proportional to  $A^{2/3}$ . Then according to (10) the multiplicity per string will fall with  $A$  as  $1/A^{2/3}$ , much faster than predicted by the colour string scenario.

So in the end we see that the old-fashioned phenomenological local pomeron model leads to predictions which do not agree with those from the fusing colour string model. The multiplicities fall too fast at high values of  $A$  and the average transverse momentum does not grow at all. It is remarkable that this situation radically changes with the perturbative QCD pomeron.

## 4 Perturbative QCD pomeron

The fundamental change introduced by the perturbative QCD approach is that the pomeron becomes non-local. Its propagation is now governed by the BFKL equation (see [14] for a review). Its interaction is realized by the triple pomeron vertex, which is also non-local [15, 16]. Equations which describe nucleus-nucleus interaction in the perturbative QCD framework have been obtained in [17]. They are quite complicated and difficult to solve (see [19] for a partial solution), but they will be not needed for our purpose. Knowing that the AGK rules are satisfied for the diagrams with BFKL pomerons interacting via the triple pomeron vertex [16] and using arguments of [12] it is easy to conclude that, as with the old local pomerons, the inclusive cross-section will again be given by the convolution of two sums of fan diagrams propagating from the emitted particle towards the two nuclei. The fundamental difference will be that the transverse momentum dependence will not be factorized as in (18) but depend non-trivially on the momenta inside the two non-local fans.

Taking again  $A = B$  and constant nuclear density for  $|b| < R_A$  we find the inclusive cross-section in the perturbative QCD as [20]

$$I_A(y, k) = A^{2/3} \pi R_0^2 \frac{8N_c \alpha_s}{k^2} \int d^2 r e^{ikr} [\Delta \Phi_A(Y - y, r)] [\Delta \Phi_A(y, r)], \quad (21)$$

where  $\Delta$  is the two-dimensional Laplacian and  $\Phi(y, r)$  is the sum of all fan diagrams connecting the pomeron at rapidity  $y$  and of the transverse dimension  $r$  with the colliding nuclei, one at rest and the other at rapidity  $Y$ . Function  $\phi_A(y, r) = \Phi(y, r)/(2\pi r^2)$ , in the momentum space, satisfies the well-known non-linear equation [6, 7, 18]

$$\frac{\partial\phi(y, q)}{\partial\bar{y}} = -H\phi(y, q) - \phi^2(y, q), \quad (22)$$

where  $\bar{y} = \bar{\alpha}y$ ,  $\bar{\alpha} = \alpha_s N_c/\pi$ ,  $\alpha_s$  and  $N_c$  are the strong coupling constant and the number of colours, respectively, and  $H$  is the BFKL Hamiltonian. Eq. (22) has to be solved with the initial condition at  $y = 0$  determined by the colour dipole distribution in the nucleon smeared by the profile function of the nucleus.

In our study we have taken the initial condition in accordance with the Golec-Biernat distribution [21], duly generalized for the nucleus:

$$\phi(0, q) = -\frac{1}{2}a \text{Ei} \left( -\frac{q^2}{0.3567 \text{ GeV}^2} \right), \quad (23)$$

with

$$a = A^{1/3} \frac{20.8 \text{ mb}}{\pi R_0^2}. \quad (24)$$

Evolving  $\phi(y, q)$  up to values  $\bar{y} = 3$  we found the inclusive cross-section (21) at center rapidity for energies corresponding to the overall rapidity  $Y = \bar{Y}/\bar{\alpha}$ . with  $\bar{Y} = 6$ . Taking  $\alpha_s = 0.2$  this gives  $Y \sim 31$ , which is far beyond the present possibilities. The overall cutoffs for integration momenta in Eq.(22) were taken according to  $0.3 \cdot 10^{-8} \text{ GeV}/c < q < 0.3 \cdot 10^{+16} \text{ GeV}/c$ .

The found inclusive cross-sections are illustrated in Figs 2-6. To see how the form of the distribution changes with energy, we present in Fig. 2 the distributions for  $A = 1$  and  $y = Y/2$  normalized to unity and multiplied by  $k^2$  to exclude the trivial  $1/k^2$  dependence present in (21),

$$J_1(y, k) = k^2 I_1(y, k) / \int \frac{d^2k}{(2\pi)^2} I_1(y, k) \quad (25)$$

at different energies corresponding to  $\bar{Y} = 1, 3, 6$ . One observes how, with the growth of energy, the distributions are shifted towards higher values of  $k$ .

In Figs. 3-6 we illustrate the  $A$ -dependence showing ratios

$$R_A^{col} = \frac{I_A(y, k)}{A^{4/3} I_1(y, k)} \quad (26)$$

and

$$R_A^{part} = \frac{I_A(y, k)}{A I_1(y, k)} \quad (27)$$

with inclusive cross-sections scaled by *the number of collisions*,  $\propto A^{4/3}$ , or by *the number of participants*  $\propto A$ , at  $y = Y/2$  and  $Y = 1, 3$  and  $6$ . One clearly sees that whereas at relatively small momenta the inclusive cross-sections are proportional to  $A$ , that is to *the number of participants*, at larger momenta they grow with  $A$  faster, however noticeably slower than the number of collisions, approximately as  $A^{1.1}$ . The interval of momenta for which  $I_A \propto A$  is growing with energy, so that one may conjecture that at infinite energies all the spectrum will be proportional to  $A$ .

Passing to the determination of both multiplicities and average transverse momenta one has to observe certain care because of the properties of the perturbative QCD solution in the leading approximation embodied in Eq. (22). As follows from (21) the inclusive cross-section

blows up at  $k^2 \rightarrow 0$  independent of the rapidity  $y$ . So the corresponding total multiplicity diverges logarithmically. However, the physical sense has only emission of jets with high enough transverse momenta. Thus we restricted ourselves to produced jets with  $k > k_{min}$ . For  $k_{min}$  we chose two possibilities:  $k_{min} = 0.3$  and  $1.0$  GeV/c. Our conclusions turned out to be practically independent of this choice. In the following we discuss the results with  $k_{min} = 0.3$  GeV/c. As to the average transverse momentum, the calculated  $\phi(y, q)$  fall very slowly with  $q$ , so that  $\langle k^2 \rangle$  clearly diverges. Even the calculation of  $\langle |k| \rangle$ , which converges, encounters certain difficulties at highest  $Y$  due to reduced precision and influence of overall cutoffs. So we found our values of average  $k^2$  squared as  $\langle |k| \rangle^2$ .

Due to unreasonably high value of the BFKL intercept  $\Delta = \bar{\alpha} 4 \ln 2$ , both the multiplicities and average transverse momenta grow very fast with  $Y$  and reach unreasonably high values  $\mu \sim 10^6$  and  $\langle |k| \rangle \sim 10^4$  GeV/c at  $\bar{Y} = 6$ . However we are not interested in the  $Y$  dependence but rather in the  $A$ -dependence, since in the fusing string scenario the energy dependence is introduced on the phenomenological grounds.

To a very good precision, at high energies corresponding to scaled rapidities  $\bar{Y} > 2$  the total multiplicities are found to be proportional to  $A$ , that is to *the number of participants*.

To compare with the string scenario we turn to multiplicities per string  $\mu_A$ . In Tables 1 and 2 the ratios

$$r_\mu(A) = \frac{\mu_A}{\mu_1}, \quad r_k(A) = \left( \frac{\langle |k| \rangle_A}{\langle |k| \rangle_1} \right)^2 \quad (28)$$

at given overall scaled rapidities  $\bar{Y} = 1, \dots, 6$ . Table 3 shows the product  $r_\mu r_k$  which is unity in the fusion strings model. These results were obtained with the low  $k_{min}$ .

Table 1: Ratios  $r_\mu(A) = \frac{\mu_A}{\mu_1}$

A	$\bar{Y}=1$	2	3	4	5	6
8	0.695	0.611	0.585	0.572	0.565	0.560
27	0.531	0.439	0.412	0.400	0.392	0.387
64	0.429	0.341	0.317	0.306	0.299	0.294
125	0.358	0.278	0.256	0.246	0.240	0.236
216	0.306	0.233	0.214	0.205	0.200	0.196

Already a superficial study of these results shows their striking similarity with the predictions based on the fusing string picture. In particular the products  $r_\mu(A)r_k(A)$  result nearly universal and close to the value unity predicted by the latter. A certain drop of this product towards higher  $A$  and  $\bar{Y}$  may be related to the neglected far tail of the momentum distribution at super-high values of  $k$ , which is absolutely irrelevant for the multiplicity but can give some contribution to  $\langle |k| \rangle$ .

A more detailed comparison can be performed using Eq. (15) derived from the string picture. We fitted the better known ratios  $r_\mu(A)$  according to this equation using  $\eta_1$  as an adjustable parameter and taking for  $\sigma_N(s)$  the experimental data well-reproduced by

$$\sigma_N = 38.3 + 0.545 \ln^2 \left( \frac{s}{122 \text{ GeV}^2} \right) \quad (29)$$

The values of  $\eta_1$  which give the best least-square fit at overall scaled rapidities  $\bar{Y} = 1, 2, \dots, 6$  are

Table 2: Ratios  $r_k(A) = \left(\frac{\langle |k| \rangle_A}{\langle |k| \rangle_1}\right)^2$ 

A	$\bar{Y}=1$	2	3	4	5	6
8	1.305	1.606	1.718	1.745	1.713	1.651
27	1.559	2.123	2.336	2.378	2.310	2.214
64	1.810	2.643	2.922	3.001	2.839	2.685
125	2.025	3.117	3.508	3.568	3.319	3.105
216	2.226	3.575	4.010	4.070	3.761	3.488

Table 3: Products  $r_\mu(A)r_k(A)$ 

A	$\bar{Y}=1$	2	3	4	5	6
8	0.907	0.982	1.004	0.998	0.967	0.924
27	0.828	0.933	0.963	0.950	0.906	0.857
64	0.776	0.902	0.926	0.917	0.848	0.790
125	0.725	0.866	0.898	0.878	0.797	0.732
216	0.681	0.834	0.858	0.834	0.751	0.684

respectively

$$\eta_1 = 0.267, 0.678, 0.931, 1.201, 1.348, 1.433$$

With these  $\eta_1$ 's we reproduce the data for  $r_\mu(A)$  from Table 1 by Eq. (15) with the average relative error which goes from the maximal 2.8% at  $\bar{Y} = 1$  down to minimal 0.98% at  $\bar{Y} = 6$ . Using the adjusted value of  $\eta_1$  at  $\bar{Y} = 1$  and assuming that at this comparatively low energy the number of strings in the  $NN$  collision is exactly 2, we could determine the effective string radius corresponding to the pomeron picture to be  $r_0 = 0.32$  fm. This value is astonishingly close to standard values used in the fusing string calculations. If we assume that this string radius is fixed independent of energy then we can find the effective average number of strings in a  $NN$  collision at higher energies. We find at  $\bar{Y} = 2, 3, \dots, 6$  respectively

$$\nu_N = 3.72, 4.31, 3.71, 2.81, 2.11$$

It is interesting that at accessible energies (up to  $\bar{Y} = 3$ ) the number of strings monotonously grows in accordance with the standard expectations, although noticeably slower. This may be interpreted as a signal of string fusion already in  $NN$  collisions. At still higher energies this phenomenon seems to become much stronger so that the effective average of strings begins to fall.

So to conclude the predictions from the perturbative QCD pomeron approach seem to fully agree with those from the fusing string picture.



## 5 Conclusions

We have compared predictions for multiplicities and average transverse momentum which follow from the semi-phenomenological fusing colour string picture for the soft domain with those which follow from the pomeron approach, both phenomenological and perturbatively derived from QCD.

The old-fashioned pomeron approach with triple pomeron interaction leads to results which disagree with the colour string models both with or without fusion. The average transverse momentum in this approach is independent of  $A$ , contrary to predictions of the colour model with fusion. On the other hand, the multiplicity per string falls with  $A$ , in contradiction with the predictions of the models without fusion. In fact the only way to reconcile the two models is to assume the eikonal form for the multiple pomeron exchange without the triple pomeron interaction. Such a model gives prediction equivalent to the independent string picture (without fusion). In fact this is the dynamics tacitly assumed in the original form of the string model [1, 2]

The perturbative QCD pomeron gives results which are in remarkable agreement with the string model with fusion. The behaviour of the multiplicities and average transverse momentum are in good agreement not only qualitatively but also quantitatively. Moreover the effective string radius extracted from these results turns out to be in agreement with the standardly assumed value in fusing colour string calculations. This overall agreement may appear to be astonishing in view of very different dynamical pictures put in the basis of the two approaches and also quite different domains of their applicability: soft for the string picture and hard for the pomeron picture. However, on second thought, one may come to the conclusion that the dynamical difference between the two approaches is not so unbridgeable. Two phenomenons are playing the leading role in both approaches. One is fusion of exchanged elemental objects, strings in one picture and pomerons in the other. This explains damping of multiplicities per one initial elemental object. Second phenomenon is the rise of average transverse momentum with this fusion. It is generated by formation of strings of higher tension (colour) in the string scenario. In the pomeron model this rise occurs due the growth of the so-called saturation momentum, which shifts the momentum distribution to higher momenta with  $A$  (and  $Y$ ). Due to this shift non-linear effects in Eq. (22) in some sense reproduce formation of strings of higher colour in the string model.

The discovered similarity in predictions between the perturbative QCD pomeron and fusing string model indicates that the dynamics of strong interaction does not radically change when passing from the soft to very hard region, in spite of the change in its microscopic content, from strings to partons. It also leaves certain hopes that these predictions are well founded in spite of all known limitations in validity and applicability of these models.

## 6 Acknowledgements

The authors are deeply indebted to N.Armesto for a constructive discussion and valuable comments. This work has been supported by a NATO Grant PST.CLG.980287, a contract FPA2002-01161 from CICYT of Spain and a contract PGIDIT03 from Galicia.

## References

- [1] A.Capella, U.P.Sukhatme, C.-I.Tan and J.Tran Thanh Van, Phys. Lett. **81** (1979) 68; Phys. Rep. **236** (1994) 225.
- [2] A.B.Kaidalov and K.A.Ter-Martirosyan, Phys. Lett. **B 117** (1982) 247.
- [3] M.A.Braun and C.Pajares, Phys. Lett. **B 287** (1992) 154; Nucl. Phys. **B 390** (1993) 542, 549.
- [4] N.Armesto, M.A.Braun, E.G.Ferreiro and C.Pajares, Phys. Rev. Lett. **77** (1996) 3736.
- [5] M.A.Braun and C.Pajares, Eur. Phys. J. **C 16** (2000) 349.
- [6] Yu.V.Kovchegov, Phys. Rev. **D 60** (1999) 034008; **D 61** (2000) 074018.
- [7] M.A.Braun, Eur. Phys. J. **C 16** (2000) 337.
- [8] L.D.McLerran, J.Schaffner-Bielich, Phys. Lett. **B 514** (2001) 29; J.Scaffner-Bielich, D.Kharzeev, L.D.McLerran and R.Venugopalan, Nucl. Phys **A 705** (2002) 494.
- [9] L.D.McLerran and R.Venugopalan, Phys. Rev. **D 49** (1994) 2233,3352; **D 50** (1994) 2225; E.G.Ferreiro, E.Iancu, A.Leonidov and L.D.McLerran, Nucl.Phys. **A 710** 5414.
- [10] N.Armesto and M.A.Braun, Eur. Phys. J **C 20** (2001) 517.
- [11] M.A.Braun, F.del Moral and C.Pajares, Phys.Rev. **C 65** (2002) 024907; J.Dias de Deus, E.G.ferreiro, C.Pajares and R.Ugoccioni, hep-ph/0304068 and Phys.Lett. **B 581** (2004) 156.
- [12] M.Ciafaloni *et al.*, Nucl. Phys. **B 98** (1975) 493.
- [13] A.Schwimmer, Nucl. Phys. **B 94** (1975) 445.
- [14] L.N.Lipatov in: Perturbative QCD, ed. A.H.Mueller (World sci., Singapore), p. 411.
- [15] A.Mueller and B.Patel, Nucl. Phys. **B 425** (1994) 471.
- [16] J.Bartels and M.Wuesthoff, Z.Physik, **C 66** (1995) 157.
- [17] M.A.Braun, Phys. Lett. **B 483** (2000) 115.
- [18] I.I.Balitsky, Nucl. Phys. **B 463** (1996) 99.
- [19] M.A.Braun, hep-ph/0309293, to be published in Eur. Phys. J. C.
- [20] M.A.Braun, Phys. Lett. **B 483** (2000) 105.
- [21] K.Golec-Biernat and M.Wuesthoff, Phys. Rev. **D 59** (1999) 014017; **D 60** (2000) 114023.

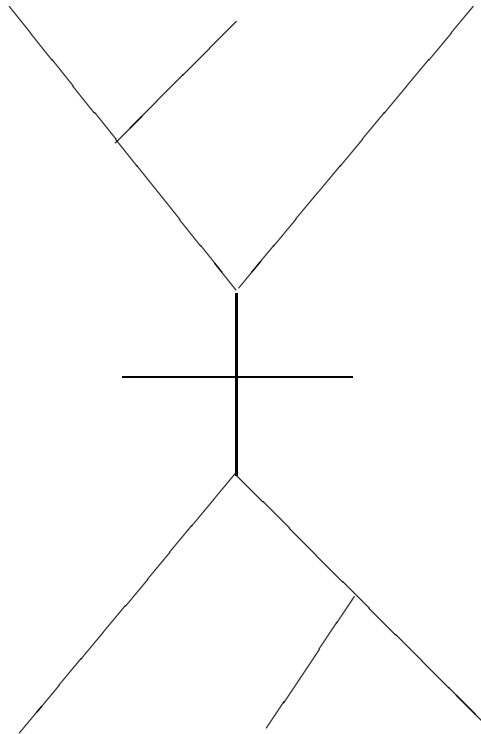


Figure 1: A typical diagram for the inclusive cross-section in nucleus-nucleus collisions.

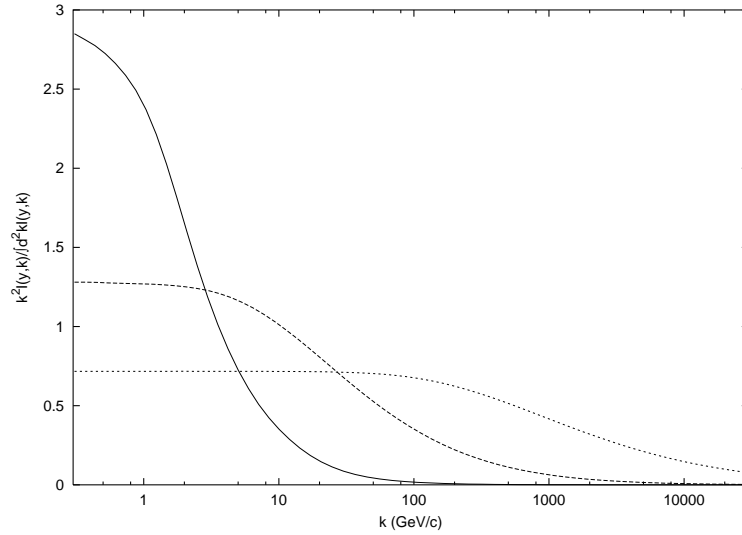


Figure 2: Normalized distributions  $J_1(y, k)$  (Eq. (25)) at  $y = \frac{Y}{2}$ . Curves from top to bottom at small  $k$  correspond to scaled overall rapidities  $\bar{Y} = 1, 3, 6$ .

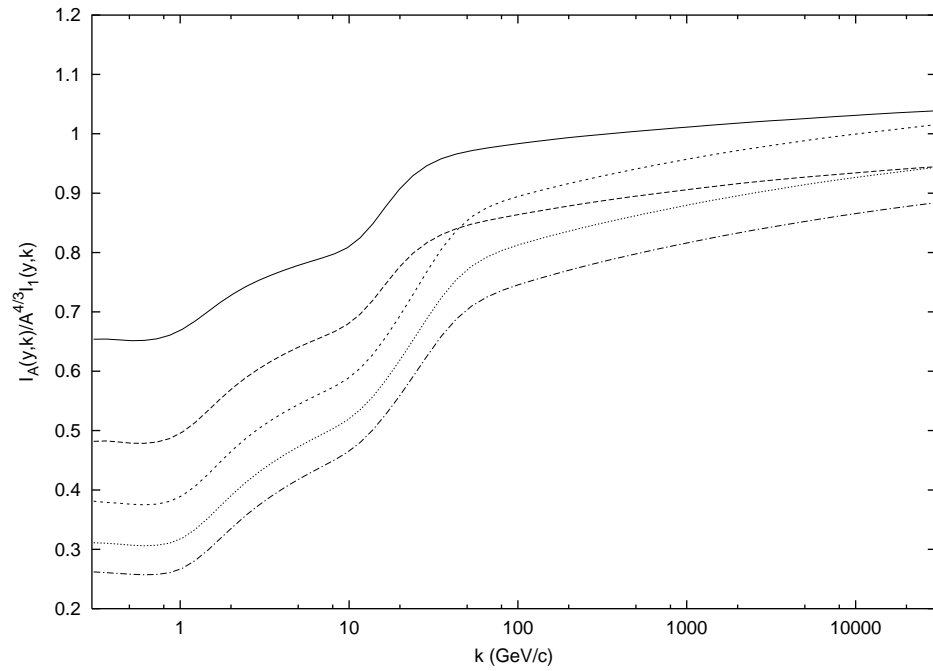


Figure 3: A-dependence of momentum distributions, scaled with the number of collisions, at  $\bar{Y} = 1$ . Curves from top to bottom show ratios  $I_A(y, k) / A^{4/3} I_1(y, k)$  at center rapidity ( $y = \frac{Y}{2}$ ) for  $A = 8, 27, 64, 125$  and  $216$ .

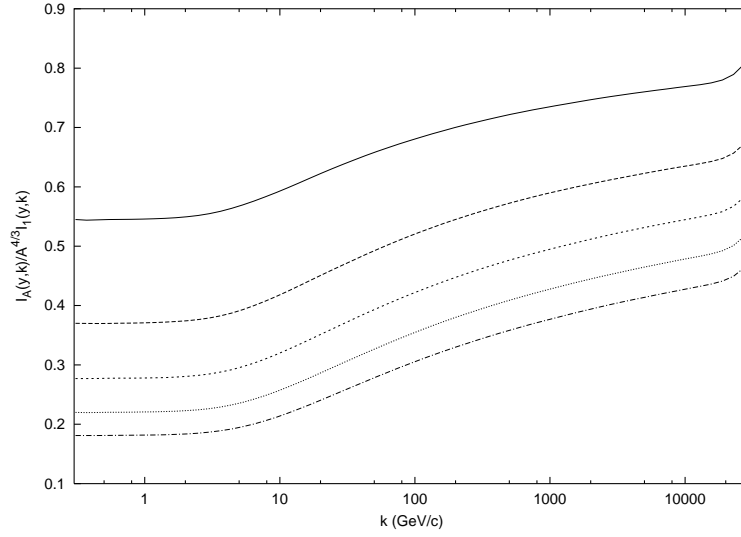


Figure 4: Same as Fig. 3 for  $\bar{Y} = 3$ .

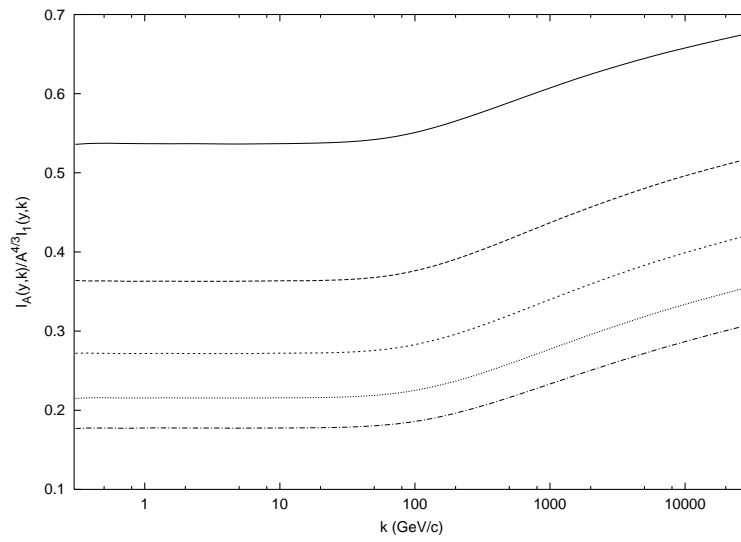


Figure 5: Same as Fig. 3 for  $\bar{Y} = 6$ .

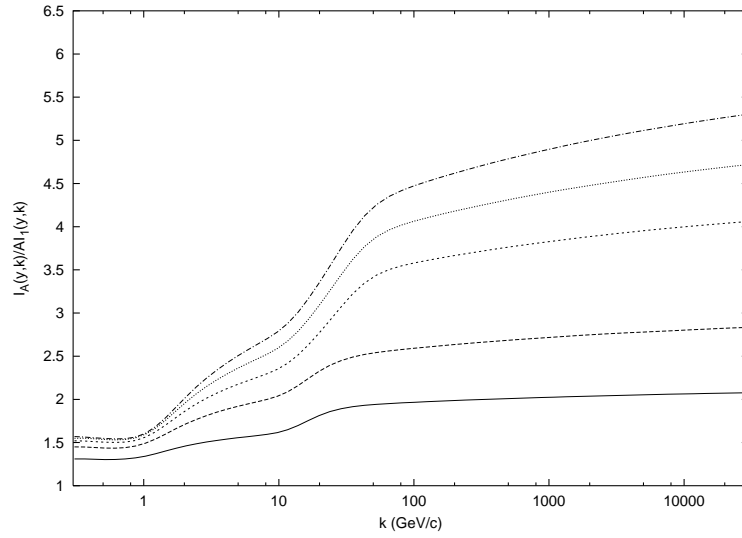


Figure 6: A-dependence of momentum distributions, scaled with the number of participants, at  $\bar{Y} = 1$ . Curves from bottom to top show ratios  $I_A(y, k)/AI_1(y, k)$  at center rapidity ( $y = \frac{Y}{2}$ ) for  $A = 8, 27, 64, 125$  and  $216$ .

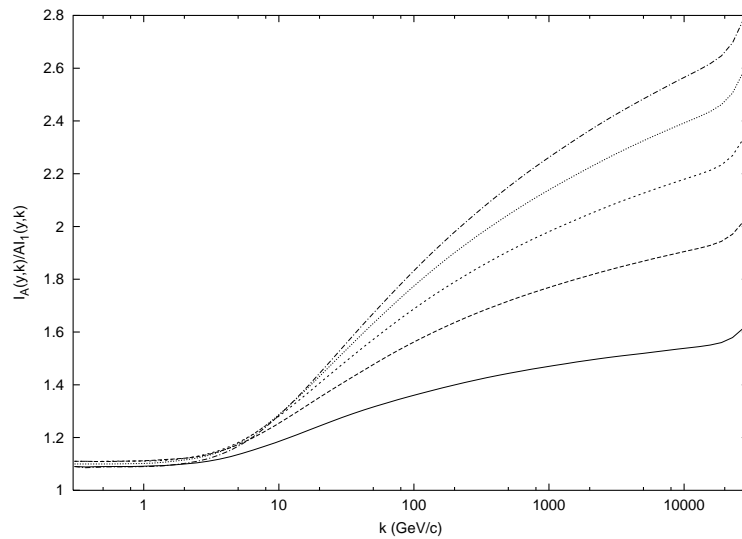


Figure 7: Same as Fig. 6 for  $\bar{Y} = 3$ .

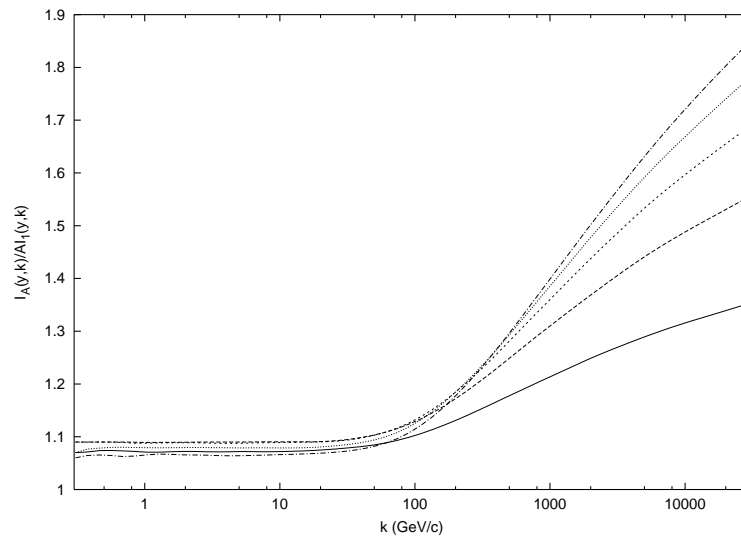


Figure 8: Same as Fig. 6 for  $\bar{Y} = 6$ .